### 4. Conclusions

An analysis has been made of the utility of integral equation theory for the study of the solvation thermodynamics of *N*-methylacetamide, a model of the peptide group in proteins. Conclusions are drawn from comparisons of two forms of the complete integral equation theory (HNC and GF) and a superposition approximation with experimental, molecular dynamics, and Monte Carlo simulation data.

The agreement in average solute–solvent (overall and group) interaction energy between the HNC/GF approximations and a molecular dynamics simulation of the same model is encouraging and provides a self-consistency test. The HNC approximation was found to be poor for the *absolute* solvation thermodynamic calculations of NMA when compared with experimental data; the values from the GF approximation were in good agreement with experiment. In light of the earlier success of the GF approximation for the aqueous solvation of nonpolar solutes, this suggests that the GF approximation is more promising overall for absolute solvation thermodynamics. The calculated relative solvation thermodynamics (cis vs trans conformers) were much less sensitive to the choice of HNC or GF free energy functionals. By analysis of the contributions to the relative solvation thermodynamics from various functional groups in NMA, it was found that correlations among groups (in particular, polar groups) can interfere with the solvation requirements of one another. As a result, the more exposed C=O and N—H in *cis*-NMA were found to have an unfavorable solvation free energy relative to that of *trans*-NMA. Such correlated interference can have important effects on protein solvation and stability. For the main chain and polar side chains, even if the solvent-accessible surface areas of the donor and acceptor groups increase or remain the same, intramolecular hydrogen-bonded conformation can be expected to be disfavored by correlation effects in aqueous solvation. The relation of these results to atomic solvation parameters[75,77] will be considered separately.[78]

The superposition approximation gives relative solvation results that are similar to the more rigorous HNC or GF approximations. Thus, the superposition approximation is likely to be useful due to its significant computational advantage over the HNC and GF integral equation theories. When the potential parameters depend on the cis and trans conformations, the cancellation of 1,2 and 1,3 contributions assumed in the superposition approximation does not occur. As expected, it fails to approximate the more rigorous integral equation theory for this case. Inclusion of the contributions from the 1,2 and 1,3 pairs in the superposition approximation improves the results. For many problems in biopolymer thermodynamics such cancellation is implicit in the choice of potential functions so that neglect of these contributions is expected to be unimportant.

The computational simplicity and the capacity of the superposition approximation to take account of pairwise correlations, and the capacity of the accessible surface area models to partly remedy the pairwise additivity assumption in the superposition approximation, make it of interest to develop a scheme that combines the two. A possible route is to scale the superposition approximation pairwise free energy by the calculated solvent-accessible surface area of the pair. This would remove the contributions of interior atoms to which the superposition approximation does not apply. It should also improve on the scheme of assigning the free energy of solvation on the basis of uncorrelated solvent-accessible surface area alone. Of particular interest may be its application to computing the entropy and other properties of peptides and denatured proteins, which cannot be studied in detail by full simulation methods at the present time. The solvent-modified potential of mean force so derived can also be combined with the empirical potential energy functions used in molecular mechanics programs to simulate complex biological macromolecules in water without the explicit presence of water molecules. Since the potential of mean force from the integral equation calculation includes only the static effect of the solvent, the dynamical solvent effects have to be included by introducing models of stochastic and dissipative forces. Such a simplified simulation approach is being compared to detailed simulations with explicit water molecules to assess its usefulness.[80]

(80) Pettitt, B. M.; Yu, H. A.; Karplus, M. to be published.

# Intrinsic Barriers of Some Model S_N2 Reactions: Second-Order Møller–Plesset Perturbation Calculations

### Zheng Shi and Russell J. Boyd*

*Contribution from the Department of Chemistry, Dalhousie University, Halifax, Nova Scotia, Canada B3H 4J3. Received April 24, 1990*

**Abstract:** Ab initio calculations including electron correlation are used to determine the factors which govern the height of the intrinsic barriers of $S_N2$ reactions. It is shown that the reactions can be classified according to the hybridization of the leaving group and the electronic structure of the transition state. A sp-hybridized atom leads to a high intrinsic barrier. A large contribution of the $N:^-$ $R^+$ $:X^-$ configuration to the transition state (in addition to its contribution to the reactant and product) lowers the intrinsic barrier. Within each group, the intrinsic barrier is related to the electronegativity of the leaving group. As the electronegativity of the leaving group increases, the intrinsic barrier decreases. Within each group there is a linear relationship between $\Delta E^{\ddagger}$ and $\Delta E^{\circ}_c$. Results are presented for $N^- + CH_3X \rightarrow CH_3N + X^-$, where X = H, CCH, CN, NC, PH_2, SH, Cl, NH_2, OH, OOH, and F for N = H; X = H, CCH, CN, NC, PH_2, SH, Cl, NH_2, OH, and F for N = F; and X = N = CCH, CN, NC, PH_2, SH, Cl, NH_2, OH, and OOH.

### Introduction

The concept of an intrinsic barrier was introduced by Marcus[1] within the framework of a theory for electron-transfer reactions.

He proposed an equation in which the free energy of activation ($\Delta G^{\ddagger}$) is related (eq 1) not only to the free energy of a reaction

$$\Delta G^{\ddagger} = \Delta G^{\ddagger}_0 + 0.5\Delta G^{\circ} + [(\Delta G^{\circ})^2/16\Delta G^{\ddagger}_0] \qquad (1)$$

($\Delta G^{\circ}$) but also to the intrinsic barrier ($\Delta G^{\ddagger}_0$). Marcus interpreted $\Delta G^{\ddagger}_0$ as the reorganization energy, i.e., the energy changes nec-

(1) (a) Marcus, R. A. *J. Phys. Chem.* **1968**, *72*, 891. (b) Cohen, A. O.; Marcus, R. A. *Ibid.* **1968**, *72*, 4249. (c) Marcus, R. A. *J. Am. Chem. Soc.* **1969**, *91*, 7224.

essary to reach the transition state (TS) by bond lengthening, compression and/or torsion, bond angle changes, and reorganization of solvent molecules. According to eq 1, $\Delta G^*_0$ equals $\Delta G^*$ when $\Delta G^°$ is zero. Thus, $\Delta G^*_0$ is the activation barrier that would exist in the absence of any thermodynamic driving force. For this reason $\Delta G^*_0$ is called the intrinsic barrier and may be thought of as the purely kinetic contribution to the reaction barrier.

The Marcus equation has been successfully used in a wide range of reactions, for example, proton-transfer reactions,[1a,b,2] hydrogen-transfer reactions,[3] and methyl-transfer reactions.[4]

The concept of an intrinsic barrier adds another dimension to the discussion of reactivities, and it provides valuable insight into the reaction process. If the intrinsic barriers for a series of reactions are similar, then the different reactivities are a direct result of different thermodynamic driving forces. However, if the intrinsic barriers are not equal, the reactivities cannot be explained in general by the thermodynamic properties. Thus, the breakdown of the rate–equilibrium relationship and the reactivity–selectivity principle can be explained in terms of the variation of the intrinsic barriers.[5] Also, the anomalous values of the Brönsted coefficient ($\alpha > 1$) can be explained by the large variation of the intrinsic barriers within a series of reactions.[1c] Accurate estimates of intrinsic barriers would enable us to predict reactivities and enhance our understanding of reaction mechanisms at the molecular level.

Previous attempts to correlate the intrinsic barriers with thermodynamic properties have been made on the basis of experimental and theoretical (HF/4-31G) data.[6] In this contribution, theoretical studies of model $S_N2$ reactions $N^- + CH_3X \rightarrow CH_3N + X^-$ (where X = H, CCH, CN, NC, PH$_2$, SH, Cl, NH$_2$, OH, OOH, and F for N = H; X = H, CCH, CN, NC, PH$_2$, SH, Cl, NH$_2$, OH, and F for N = F; and X = N = CCH, CN, NC, PH$_2$, SH, Cl, NH$_2$, OH, and OOH) are presented. The intention is to provide a molecular understanding of the factors which determine the height of the intrinsic barrier. The results are compared with the predictions of the Shaik–Pross model, and the rate–equilibrium relationship is discussed.

### Computational Methods

In earlier papers of our series on gas-phase $S_N2$ reactions,[7] we have described the computational methods and results obtained at three levels of sophistication.[7b,c] In this paper, the method denoted by MP2' in previous papers is used.[7] That is, the geometries were optimized at the HF level using the analytic gradient method, and energies were calculated by use of second-order Møller–Plesset perturbation theory. Details about optimized geometries and energies can be found elsewhere.[7b,c] The 6-31G basis set supplemented with diffuse and polarization functions (standard notation 6-31++G**) was used for all atoms except the three methyl hydrogens for which the 6-31G basis set was used. The justification for using single-point Møller–Plesset calculations carried out at the geometries optimized at the HF level has been discussed in previous papers.[7b–d] It has been shown that for those properties which involve at least two states, for example, energy differences and contribution analysis of the TS, the MP2' method gives results which are consistent with the full MP2 treatment (second-order Møller–Plesset perturbation calculations carried out at the geometries optimized at the same level).

The calculations were done by using the GAUSSIAN 80 and GAUSSIAN 86 programs[8] and the topological properties were calculated using the

**Table I.** Intrinsic Barriers, Activation Barriers, and Reaction Energies at the MP2' Level (kJ/mol)

| $N^- + RX^a$ | $\Delta E^*_{0(NX)}$ | $\Delta E^*$ | $\Delta E^°_c$ |
|---|---|---|---|
| H$^-$ + RCCH | 231.56 | 172.35 | -127.13 |
| H$^-$ + RCN | 218.34 | 127.25 | -206.61 |
| H$^-$ + RNC | 182.45 | 60.83 | -308.41 |
| H$^-$ + RPH$_2$ | 190.20 | 108.07 | -187.31 |
| H$^-$ + RSH | 173.73 | 56.50 | -275.74 |
| H$^-$ + RCl | 136.97 | 15.35 | -364.49 |
| H$^-$ + RNH$_2$ | 191.90 | 150.45 | -87.92 |
| H$^-$ + ROH | 163.51 | 87.14 | -176.57 |
| H$^-$ + ROOH | 152.95 | 68.03 | -203.77 |
| H$^-$ + RF | 129.72 | 32.93 | -257.47 |
| F$^-$ + RCCH | 122.55 | 200.79 | 137.26 |
| F$^-$ + RCN | 117.52 | 153.94 | 67.92 |
| F$^-$ + RNC | 92.00 | 76.26 | -32.97 |
| F$^-$ + RPH$_2$ | 103.12 | 147.14 | 80.23 |
| F$^-$ + RSH | 83.60 | 79.79 | -7.70 |
| F$^-$ + RCl | 63.31 | 25.13 | -93.71 |
| F$^-$ + RNH$_2$ | 92.70 | 188.95 | 158.58 |
| F$^-$ + ROH | 74.18 | 115.85 | 74.09 |

$^a$ R = CH$_3$.

PROAIM and modified PROAIM packages.[9]

### Results and Discussion

Gas-phase $S_N2$ reactions involve three steps:[4d,10]

$$N^- + CH_3X = N^-\cdots CH_3X = NCH_3\cdots X^- = CH_3N + X^- \quad (2)$$

The second step, the conversion of the reactant ion–molecule complex to the product ion–molecule complex, determines the efficiency of the reaction.[4d,10a] In this work, the Marcus equation is used to analyze this elementary step. Thus, the reactant and product are referred to as $N^-\cdots CH_3X$ and $NCH_3\cdots X^-$, respectively, unless stated otherwise. The corresponding potential energy form of the Marcus equation[1a] for this elementary reaction is

$$\Delta E^* = \Delta E^*_0 + 0.5\Delta E^°_c + [(\Delta E^°_c)^2/16\Delta E^*_0] \quad (3)$$

where $\Delta E^°_c = E(NCH_3\cdots X^-) - E(N^-\cdots CH_3X)$ is the reaction energy, $\Delta E^*$ is the energy barrier for this elementary reaction, and $\Delta E^*_0$ is the intrinsic barrier of the elementary reaction.

**Intrinsic Barriers of Asymmetric Reactions.** The intrinsic barrier for a symmetric reaction can be understood intuitively since $\Delta E^*_0$ is equal to $\Delta E^*$ for a symmetric reaction. For an asymmetric reaction, however, the meaning of the intrinsic barrier is not obvious. Nevertheless, if $|\Delta E^°_0|$ is small compared to $\Delta E^*_0$, the quadratic term in eq 3 can be neglected. Thus, if the activation energy for the forward reaction is denoted by $\Delta E^*_f$ and that for the reverse reaction by $\Delta E^*_r$, then

$$\Delta E^*_f + \Delta E^*_r = 2\Delta E^*_0 + [(\Delta E^°_c)^2/8\Delta E^*_0] \approx 2\Delta E^*_0 \quad (4)$$

and we see that the intrinsic barrier of an asymmetric reaction is the average activation energy of the forward and reverse reactions. Thus, in order for $N^-$ to be a good nucleophile and for $X^-$ to be simultaneously a good leaving group, the reaction must have a small intrinsic barrier.

For asymmetric reactions, $\Delta E^*_0$ can be calculated from eq 3 directly if $\Delta E^*$ and $\Delta E^°_c$ are known or $\Delta E^*_0$ can be approximated by eq 5[1a,b]

$$\Delta E^*_{0(XY)} = 0.5(\Delta E^*_{0(XX)} + \Delta E^*_{0(YY)}) \quad (5)$$

where $\Delta E^*_{0(XX)}$ and $\Delta E^*_{0(YY)}$ are intrinsic barriers of the corre-

(2) (a) Bell, R. P. *The Proton in Chemistry*, 2nd ed.; Chapman and Hall: London, 1973. (b) Caldin, E., Gold, V., Eds. *Proton Transfer Reactions*; Chapman and Hall: London, 1973. (c) Kreevoy, M. M.; Oh, S.-W. *J. Am. Chem. Soc.* **1973**, *95*, 4805. (d) Kresge, A. *Chem. Soc. Rev.* **1973**, *2*, 475.

(3) Kreevoy, M. M.; Han Lee, I.-S. *J. Am. Chem. Soc.* **1984**, *106*, 2550.

(4) (a) Albery, W. J.; Kreevoy, M. M. *Adv. Phys. Org. Chem.* **1978**, *16*, 87. (b) Albery, W. J. *Annu. Rev. Phys. Chem.* **1980**, *31*, 227. (c) Lewis, E. S.; Kukes, S.; Slater, C. D. *J. Am. Chem. Soc.* **1980**, *102*, 1619. (d) Pellerite, M. J.; Brauman, J. I. *Ibid.* **1980**, *102*, 5993.

(5) Shaik, S. S. *Prog. Phys. Org. Chem.* **1985**, *15*, 197.

(6) (a) Pellerite, M. J.; Brauman, J. I. *J. Am. Chem. Soc.* **1983**, *105*, 2672. (b) Brauman, J. I.; Dodd, J. A.; Han, C. C. In *Nucleophilicity*; Harris, J. M., McManus, S. P., Eds.; Advances in Chemistry Series 215; American Chemical Society: Washington, DC, 1987; p 23. (c) Mitchell, D. J.; Schlegel, H. B.; Shaik, S. S.; Wolfe, S. *Can. J. Chem.* **1985**, *63*, 1642.

(7) Shi, Z.; Boyd, R. J. *J. Am. Chem. Soc.* **1989**, *111*, 1575. (b) Shi, Z. Electronic and Structural Properties of Model $S_N2$ Reactions. Ph.D. Thesis, Dalhousie University, 1989. (c) Shi, Z.; Boyd, R. J. *J. Am. Chem. Soc.* **1990**, *112*, 6789. (d) Shi, Z.; Boyd, R. J. *J. Am. Chem. Soc.*, in press.

(8) (a) Binkley, J. S.; Whiteside, R. A.; Krishnan, R.; Seeger, R.; DeFrees, D. J.; Schlegel, H. B.; Topiol, S.; Kahn, L. R.; Pople, J. A. *GAUSSIAN 80*; Carnegie-Mellon Quantum Chemistry Publishing Unit: Pittsburgh, PA, 1980. (b) Frisch, M. J.; Binkley, J. S.; Schlegel, H. B.; Raghavachari, K.; Melius, C. F.; Martin, R. L.; Stewart, J. J. P.; Bobrowicz, F. W.; Rohlfing, C. M.; Kahn, L. R.; DeFrees, D. J.; Seeger, R.; Whiteside, R. A.; Fox, D. J.; Fleuder, E. M.; Pople, J. A. *GAUSSIAN 86*; Carnegie-Mellon Quantum Chemistry Publishing Unit: Pittsburgh, PA, 1984.

(9) (a) Biegler-König, F. W.; Bader, R. F. W.; Tang, T. *J. Comput. Chem.* **1982**, *3*, 317. (b) Boyd, R. J.; Wang, L. C. *J. Comput. Chem.* **1989**, *10*, 367.

(10) (a) Olmstead, W. N.; Brauman, J. I. *J. Am. Chem. Soc.* **1977**, *99*, 4219. (b) Asubiojo, O. I.; Brauman, J. I. *Ibid.* **1979**, *101*, 3715.
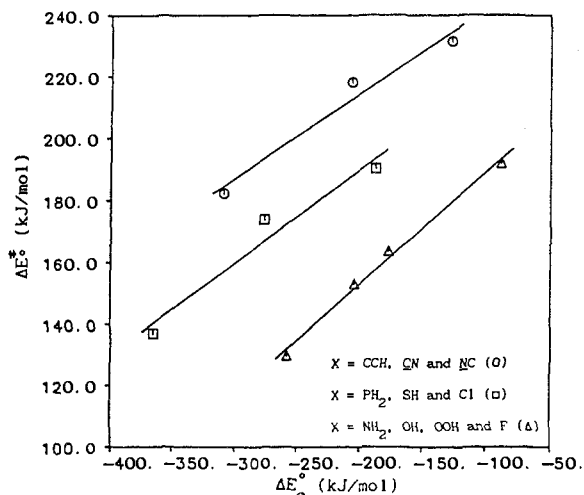
**Figure 1.** Plot of $\Delta E^{\ast}_{0}$ versus $\Delta E^{\circ}_{c}$ for $H^{-} + CH_3X \rightarrow CH_4 + X^{-}$.
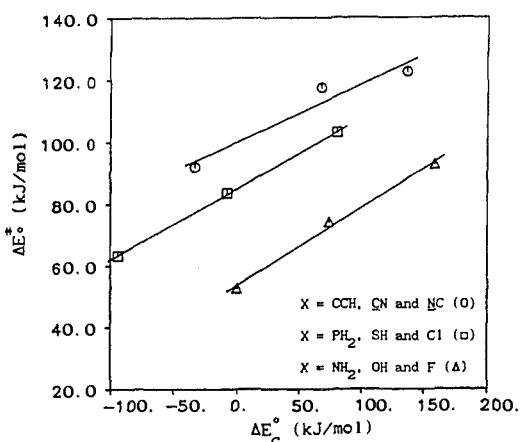


**Figure 2.** Plot of $\Delta E^{\ast}_{0}$ versus $\Delta E^{\circ}_{c}$ for $F^{-} + CH_3X \rightarrow CH_3F + X^{-}$.
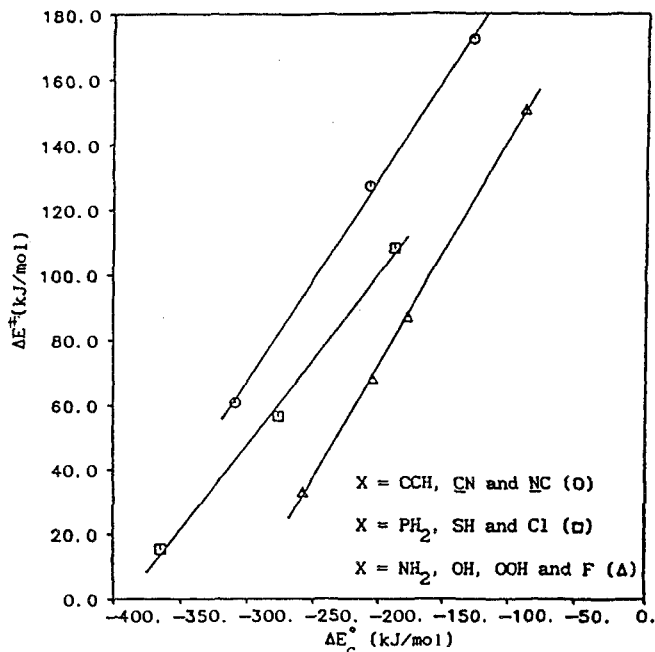


**Figure 3.** Plot of $\Delta E^{\ast}$ versus $\Delta E^{\circ}_{c}$ for $H^{-} + CH_3X \rightarrow CH_4 + X^{-}$.

sponding symmetric reactions. Table I provides values of $\Delta E^{\ast}_{0}$ calculated by means of eq 3 together with $\Delta E^{\ast}$ and $\Delta E^{\circ}_{c}$ values. Obviously, the $\Delta E^{\ast}_{0}$ values differ from one reaction to another. Also from eq 3, it is clear that a linear relationship between $\Delta E^{\ast}$ and $\Delta E^{\circ}_{c}$ (in a small segment) implies either that $\Delta E^{\ast}_{0}$ is a constant or that $\Delta E^{\ast}_{0}$ is linearly related to $\Delta E^{\circ}_{c}$. To test the latter,
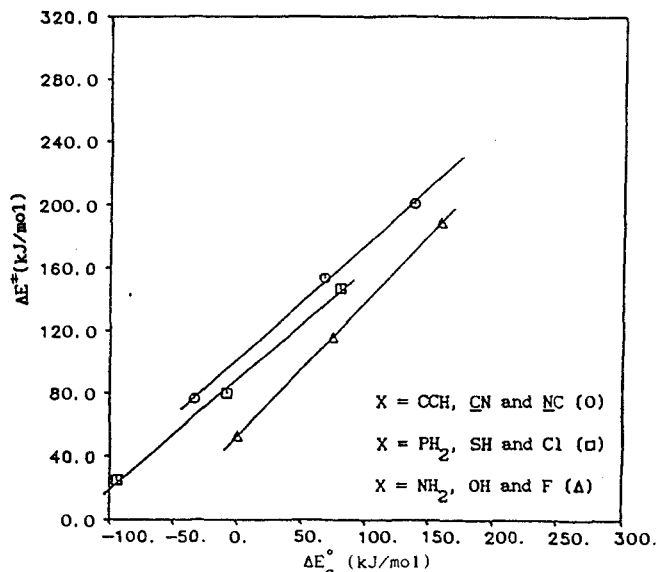


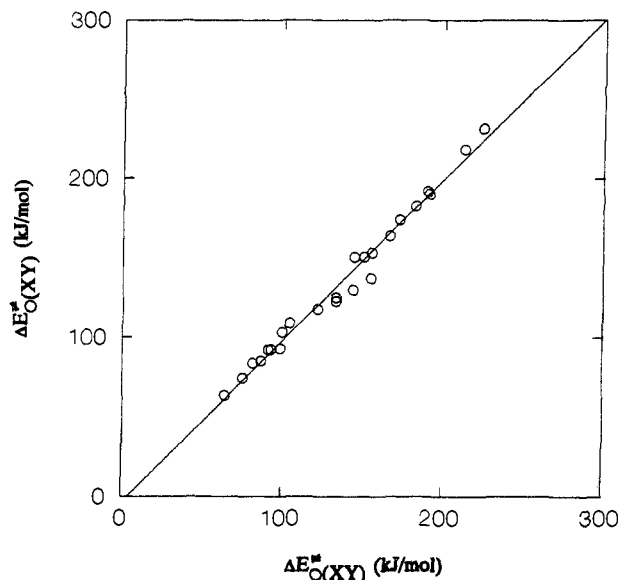**Figure 4.** Plot of $\Delta E^{\ast}$ versus $\Delta E^{\circ}_{c}$ for $F^{-} + CH_3X \rightarrow CH_3F + X^{-}$.



**Figure 5.** Plot of $\Delta E^{\ast}_{0(XY)}$ from eq 3 versus $\Delta E^{\ast}_{0(XY)}$ from eq 5. The asymmetric systems shown are: for N = H, X = CCH, $CN$, $NC$, $PH_2$, SH, Cl, $NH_2$, OH, OOH, and F; for N = F, X = CCH, $CN$, $NC$, $PH_2$, SH, Cl, $NH_2$, and OH; for N = HO, X = $CN$, SH, and Cl; for N = SH, X = $CN$ and Cl; for N = Cl, X = $CN$.

plots of $\Delta E^{\ast}_{0}$ versus $\Delta E^{\circ}_{c}$ are shown in Figures 1 and 2 for nucleophiles $H^{-}$ and $F^{-}$, respectively. In each case the reactions separate into three groups. Within each group, $\Delta E^{\ast}_{0}$ varies linearly with $\Delta E^{\circ}_{c}$. Thus, X = CCH, $CN$, and $NC$, belong to the first group, X = $PH_2$, SH, and Cl to the second group, and X = $NH_2$, OH, OOH, and F to the third group.
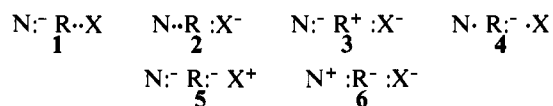
As we discussed above, if $\Delta E^{\ast}_{0}$ and $\Delta E^{\circ}_{c}$ are linearly related for a series of reactions, then $\Delta E^{\ast}$ and $\Delta E^{\circ}_{c}$ are linearly related. This is illustrated in Figures 3 and 4 for N = H and N = F, respectively. Thus, as in Figures 1 and 2, three groups of linear plots are observed in Figures 3 and 4, respectively.

The linear relationship between $\Delta E^{\ast}_{0}$ and $\Delta E^{\circ}_{c}$ shows that within each group the two quantities depend on the same variables, namely, the C–X bond energy and the electron affinity of $X^{5,11}$ which are, in turn, related to the electronegativity of X. For each group, the $\Delta E^{\ast}_{0}/\Delta E^{\circ}_{c}$ relationship has a characteristic slope and intercept which are due to the electronic structures of the reactants, transition states, and products. The classification of reaction groups is discussed below.

(11) Streitwieser, A., Jr. *Proc. Natl. Acad. Sci. U.S.A.* **1985**, *82*, 8288.

*Intrinsic Barriers of Model S$_N$2 Reactions*

*J. Am. Chem. Soc., Vol. 113, No. 7, 1991* 2437

The behavior of CCH, CN, and NC has been noted by Brauman et al. and explained in terms of hybrid orbitals.[6a,12] As we will see later, a more precise classification reveals that there are two groups within CCH, CN, and NC. One group contains CCH and CN and the other group contains NC. At this point, however, it is convenient to discuss them as one group as they all involve the same hybridization. The CCH, CN, and NC groups bond through sp-hybridized atoms, whereas the other groups use sp³-hybridized atoms for bonding. Hydrogen is a special case, since it only has one occupied s orbital. The concept of hybridization provides a simple picture of the bond arrangement and electron distribution around an atom. The hybridization affects the electronegativity of an atom and its bond energies,[13] and, therefore, it is not unexpected that the hybridization factor affects the shape of the potential energy surface and hence the relationship between $\Delta E^{\ast}_0$ and $\Delta E^{\circ}_c$.

The differences between the second and the third groups can be explained in terms of their electronic structures in the TS. There are six important valence bond configurations in S$_N$2 reactions[5,14]

$$N{:}^- \; R{\cdots}X \qquad N{\cdots}R \; {:}X^- \qquad N{:}^- \; R^+ \; {:}X^- \qquad N{\cdot} \; R{:}^- \; {\cdot}X$$
$$\mathbf{1} \qquad\qquad \mathbf{2} \qquad\qquad \mathbf{3} \qquad\qquad \mathbf{4}$$
$$N{:}^- \; R{:}^- \; X^+ \qquad N^+ \; {:}R^- \; {:}X^-$$
$$\mathbf{5} \qquad\qquad \mathbf{6}$$

According to the valence bond configuration mixing model,[5,14] the TS wave function can be written as a linear combination of these valence bond configurations

$$\Psi_{TS} = c_1\psi_1 + c_2\psi_2 + c_3\psi_3 + c_4\psi_4 \qquad (6)$$

($\psi_5$ and $\psi_6$ are omitted from eq 6 since they have higher energies and make relatively small contributions to the TS). The TS wave function can also be approximated in terms of reactant ($\Psi_r$) and product ($\Psi_p$) wave functions[7a,b,d]

$$\Psi_{TS} = a\Psi_r + b\Psi_p + c\psi_3 + d\psi_4 \qquad (7)$$

where

$$\Psi_r = a_1\psi_1 + a_2\psi_3 + a_3\psi_5 \qquad (8)$$

$$\Psi_p = b_1\psi_2 + b_2\psi_3 + b_3\psi_6 \qquad (9)$$

It should be stressed that the contribution of $\psi_3$ in eq 7 is an excess contribution of $\psi_3$ to the TS in addition to its contribution to the reactant and product. This should not be confused with the total contribution of $\psi_3$ to the TS which is the sum of $c$, $aa_2$ and $bb_2$ (see eq 7, 8, and 9).

A method, which employs the integrated charges of various configurations, has been proposed to analyze the contributions of these wave functions to the TS.[7a,b] The results (see Table II) indicate that for X = NH$_2$, OH, OOH, F, and NC the contribution of $\psi_3$ in eq 7 is small, whereas for others the contribution of $\psi_3$ is substantial (especially for N = H). Actually, the group with sp-hybridized atoms, CCH, CN, and NC, is a combination of two groups which have different electronic structures at their transition states; i.e., one group contains CCH and CN while the other group contains only X = NC. It would be desirable to include more leaving groups which like NC are sp-hybridized and have large electronegativity. However, it is difficult to identify such groups which are computationally manageable.

How does the additional contribution of a VB configuration at the TS affect the intrinsic barrier, and hence, the classification of groups? To discuss this question, it is helpful to use the concept of disparity of progress proposed by Grunwald.[16]

**Table II.** Configuration Analysis at the MP2' Level[a]

| [N···R···X]⁻ | $a^2$ | $b^2$ | $c^2$ | $d^2$ |
|---|---|---|---|---|
| [H···R···H]⁻ | 0.45 | 0.45 | 0.10 | 0.00 |
| [H···R···NH$_2$] | 0.55 | 0.42 | 0.03 | 0.00 |
| [H···R···OH] | 0.61 | 0.34 | 0.00 | 0.05 |
| [H···R···OOH] | 0.63 | 0.32 | 0.00 | 0.05 |
| [H···R···F] | 0.65 | 0.31 | 0.00 | 0.04 |
| [H···R···NC] | 0.68 | 0.28 | 0.00 | 0.04 |
| [H···R···CCH] | 0.47 | 0.39 | 0.14 | 0.00 |
| [H···R···CN] | 0.50 | 0.37 | 0.13 | 0.00 |
| [H···R···PH$_2$] | 0.36 | 0.41 | 0.24 | 0.00 |
| [H···R···SH] | 0.48 | 0.35 | 0.17 | 0.00 |
| [H···R···Cl] | 0.60 | 0.26 | 0.14 | 0.00 |
| [F···R···NH$_2$] | 0.36 | 0.59 | 0.00 | 0.05 |
| [F···R···OH] | 0.42 | 0.51 | 0.00 | 0.07 |
| [F···R···F] | 0.47 | 0.47 | 0.00 | 0.07 |
| [F···R···NC] | 0.47 | 0.48 | 0.00 | 0.05 |
| [F···R···CCH] | 0.37 | 0.62 | 0.00 | 0.02 |
| [F···R···CN] | 0.40 | 0.59 | 0.00 | 0.01 |
| [F···R···PH$_2$] | 0.29 | 0.66 | 0.05 | 0.00 |
| [F···R···SH] | 0.42 | 0.56 | 0.03 | 0.00 |
| [F···R···Cl] | 0.54 | 0.40 | 0.06 | 0.00 |
| [HO···R···OH] | 0.46 | 0.46 | 0.00 | 0.08 |
| [NC···R···CN] | 0.46 | 0.46 | 0.09 | 0.00 |
| [HS···R···SH] | 0.38 | 0.38 | 0.24 | 0.00 |
| [Cl···R···Cl] | 0.39 | 0.39 | 0.23 | 0.00 |

[a] The results presented in the table are obtained by using N⁻ + CH$_3$X and CH$_3$N + X⁻ as reactant and product, respectively. See footnote 15 for further details.

According to Grunwald, for a reaction which has two progress variables, for example, bond breaking and bond making, the TS can be displayed on a two-dimensional diagram such as the More O'Ferrall diagram.[17] The progress that corresponds to the transformation of reactant to product is called the main reaction, while the transformation of one intermediate into the other is called the disparity reaction. The alternative intermediates are formed when the reaction events occur stepwise, for example, bond breaking followed by bond making, or bond making followed by bond breaking. Thus, for a S$_N$2 reaction, the reactant and product are located at the lower left and upper right corners of the two-dimensional diagram, respectively, whereas the cationic methyl (N:⁻ R⁺ :X⁻) and anionic methyl (N· R:⁻ ·X) intermediates are located at the upper left and lower right corners, respectively.[18] If the TS wave function consists of mainly reactant and product contributions (that is, small $c$ and $d$ coefficients in eq 7), the TS is located on the diagonal line connecting the reactant and product, and the disparity index is close to zero. If the TS wave function consists of a significant contribution from configurations other than the reactant and product (that is, large $c$ or $d$ coefficients in eq 7), the TS is located off the diagonal line and the disparity index is not close to zero. Grunwald showed that the disparity of progress affects the energy barrier ($\Delta E^{\ast}$), and, hence, it affects the intrinsic barrier calculated from eq 3. Thus, the TS electronic structure affects the intrinsic barrier; the latter may be used to classify the reactions into groups.

**Intrinsic Barriers of Symmetric Reactions.** The intrinsic barrier of a symmetric reaction is an important property. According to eq 5, if the intrinsic barriers of two symmetric reactions are known, the intrinsic barrier of the corresponding asymmetric reaction can be obtained immediately.[19] Moreover, the energy barrier $\Delta E^{\ast}$ can be calculated from eq 3.

(12) Han, C. C.; Dodd, J. A.; Brauman, J. I. *J. Phys. Chem.* **1986**, *90*, 471.

(13) Huheey, J. E. *Inorganic Chemistry*, 2nd ed.; Harper & Row: New York, 1978; pp 142, 167.

(14) (a) Shaik, S. S. *J. Am. Chem. Soc.* **1981**, *103*, 3692. (b) Pross, A.; Shaik, S. S. *Ibid.* **1981**, *103*, 3702. (c) Shaik, S. S.; Pross, A. *J. Am. Chem. Soc.* **1982**, *104*, 2708. (d) Pross, A.; Shaik, S. S. *Acc. Chem. Res.* **1983**, *16*, 363. (f) Pross, A. *Adv. Phys. Org. Chem.* **1985**, *21*, 99.

(15) The electronic structures of N⁻ + CH$_3$X and N⁻···CH$_3$X are very similar (in terms of $\psi_1$, $\psi_3$, and $\psi_5$ contributions), and the same is true for NCH$_3$ + X⁻ and NCH$_3$···X⁻. Thus, the TS configuration analysis (eq 7) in terms of $\Psi_r = \Psi$(N⁻ + CH$_3$X) and $\Psi_p = \Psi$(CH$_3$N + X⁻) is similar to $\Psi_r = \Psi$(N⁻···CH$_3$X) and $\Psi_p = \Psi$(NCH$_3$···X⁻); see Tables 3.4.5 and 3.4.7 in ref 7b.

(16) Grunwald, E. *J. Am. Chem. Soc.* **1985**, *107*, 125.

(17) (a) Thornton, E. R. *J. Am. Chem. Soc.* **1967**, *89*, 2915. (b) More O'Ferrall, R. A. *J. Chem. Soc. B* **1970**, 274.

(18) (a) Lewis, E. S. *J. Phys. Chem.* **1986**, *90*, 3756. (b) Lee, I.; Seo, H. S. *Bull. Korean Chem. Soc.* **1986**, *7*, 448.

(19) Discussions about the validity of eq 5 can be found in ref 1b, 18, and 23. According to Marcus, the additivity of eq 5 is expected to hold best when the intrinsic barriers of symmetric reactions are not near zero. We compare the intrinsic barriers of asymmetric reactions ($\Delta E^{\ast}_{0(XY)}$) obtained by eq 3 and 5 in Figure 5. For eq 3, we use $\Delta E^{\ast}_{(XY)}$ and $\Delta E^{\circ}_{c(XY)}$ values from ab initio calculations. For eq 5, we use $\Delta E^{\ast}_{0(XX)}$ and $\Delta E^{\ast}_{0(YY)}$ values from ab initio calculations. For the 24 asymmetric reactions calculated, the correlation is generally good.

**Table III.** Calculated $\tau$ Values for $CH_3X$ and Intrinsic Barriers of Symmetric Reactions $X^- + CH_3X \rightarrow X^- + CH_3X$ (au) at the MP2' Level[a]

| $RX^b$ | $\Delta E^*_{0(XX)}$ | $\tau$ |
|---|---|---|
| RH | 0.08956 | 0.364 |
| RCCH | 0.08144 | 0.341 |
| RCN | 0.07275 | 0.328 |
| RNC | 0.04961 | 0.234 |
| RPH$_2$ | 0.05624 | 0.327 |
| RSH | 0.04221 | 0.296 |
| RCl | 0.02873 | 0.267 |
| RNH$_2$ | 0.05534 | 0.305 |
| ROH | 0.03751 | 0.245 |
| ROOH | 0.02908 | 0.238 |
| RF | 0.02007 | 0.216 |

[a] The intrinsic barriers are from direct ab initio calculations ($\Delta E^*_{0(XX)} = \Delta E^*_{(XX)}$) of ref 7b,c and this work. [b] R = $CH_3$.
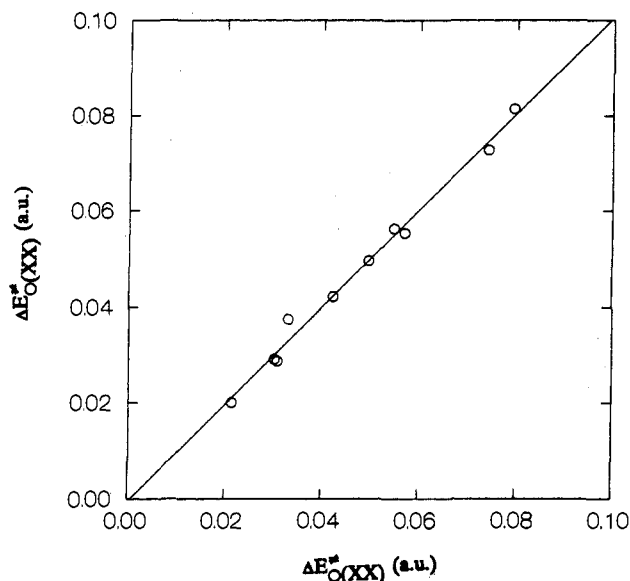
In this section we propose a method for predicting the intrinsic barriers of symmetric reactions ($\Delta E^*_{0(XX)}$) based on the topological properties of $CH_3X$. We give a brief introduction to the topological properties of electron distributions. More detailed accounts can be found elsewhere.[20] The essential topological properties of the electron density can be summarized by the complete specification of its critical points at which $\nabla \rho = 0$. Each critical point can be classified according to its rank and signature ($\lambda$, $\sigma$). The rank $\lambda$ of a critical point equals the number of nonzero eigenvalues of the Hessian matrix of electron density, while the signature $\sigma$ is the algebraic sum of the signs of the eigenvalues. A (3, –1) critical point has two negative and one positive eigenvalues. The two eigenvectors associated with the negative eigenvalues define a surface on which the critical point is a local maximum. The eigenvector associated with the positive eigenvalue defines a unique axis along which the charge density decreases for motion towards the critical point. A (3, –1) critical point appears between every pair of neighboring bonded atoms and is therefore called a bond critical point. We define a topological $\tau$ value,

$$\tau = \rho r_c \tag{10}$$

where $\rho$ is the electron density at the position of the C–X bond critical point in $CH_3X$ and $r_c$ is the distance between carbon and the bond critical point. Studies[21] have shown that the electron density at a bond critical point provides information about the type of bond: the smaller $\rho$ the greater the ionic character of the bond. Also the distance $r_c$ provides information about the relative electronegativities of the bonded atoms. A bond between C and a more electronegative X results in a small $\rho$ and a small $r_c$, and hence a small $\tau$. The calculated $\Delta E^*_{0(XX)}$ and topological $\tau$ values in Table III indicate that the $\Delta E^*_{0(XX)}$'s are related to $\tau$ values within each group of reactions. Thus, it is possible to estimate an intrinsic barrier from the $\tau$ value and the type of reaction. For this purpose the following equation is proposed

$$\Delta E^*_{0(XX)} = 0.4\tau - \omega \tag{11}$$

where $\omega$ is characteristic of each group. The groups are classified according to the type of hybridization and the electronic structure of the transition state. The best correlation between $\Delta E^*_{0(XX)}$ from eq 11 and $\Delta E^*_{0(XX)}$ from direct ab initio calculation (Table III) is obtained with the following $\omega$ values (in au): for group I (X = CCH and CN), $\omega = 0.05671$; for group II (X = NC), $\omega = 0.04399$; for group III (X = PH$_2$, SH, and Cl), $\omega = 0.07627$; and for group IV (X = NH$_2$, OH, OOH, and F), $\omega = 0.06489$. The $\Delta E^*_{0(XX)}$ values calculated by use of eq 11 are compared with the values obtained directly from ab initio calculations in Figure 6. The correlation is strong (R = 0.995). Thus, as long as the

(20) (a) Bader, R. F. W.; Tal, Y.; Anderson, S. G.; Nguyen-Dang, T. T. *Isr. J. Chem.* **1980**, *19*, 8. (b) Bader, R. F. W.; Nguyen-Dang, T. T. *Adv. Quantum Chem.* **1981**, *14*, 63. (c) Bader, R. F. W.; Nguyen-Dang, T. T.; Tal, Y. *Rep. Progr. Phys.* **1981**, *44*, 893.
(21) (a) Bader, R. F. W.; Tang, T.; Tal, Y.; Biegler-König, F. W. *J. Am. Chem. Soc.* **1982**, *104*, 946. (b) Wiberg, K. B.; Bader, R. F. W.; Lau, C. D. H. *Ibid.* **1987**, *109*, 985. (c) Boyd, R. J.; Edgecombe, K. E. *J. Am. Chem. Soc.* **1988**, *110*, 4182.



**Figure 6.** Plot of $\Delta E^*_{0(XX)}$ from ab initio calculations (Table III) versus $\Delta E^*_{0(XX)}$ from eq 11.

ground-state $\tau$ value is available, it is possible to predict $\Delta E^*_0$. For example, the $\tau$ values for $CH_2Cl_2$, $CHCl_3$, and $CCl_4$, which are not part of the present study, are 0.278, 0.296, and 0.309, respectively, at the HF level, while at the same level $\tau$ for $CH_3Cl$ is 0.254. Since they all belong to the same group, $\Delta E^*_0$ increases as $\tau$ increases. This prediction is consistent with experimental observations in solution[22] and with the predictions of Shaik and Pross.[5,14c]

According to eq 11, large $\omega$ and small $\tau$ result in a low intrinsic barrier. The $\omega$ values depend on the electronic structure of the TS and the hybridization factor of X. If the electronic structures at the TS are similar, then $\omega$ is small for those X which are sp-hybridized (for example, group I has a smaller $\omega$ than group III and group II has a smaller $\omega$ than group IV). If the hybridization factor is the same, $\omega$ is large for those groups in which $\psi_3$ makes an additional contribution to the transition state (i.e., $c$ in eq 7 is substantial or the disparity of progress is significant). For example, groups III and IV (also groups I and II) have the same hybridization factor; however, because of the additional contribution of $\psi_3$ to the TS (see the symmetric reactions in Table II and remember that $c$ is not the total contribution of $\psi_3$ to the TS), group III has a larger $\omega$ (0.076 27) than group IV (0.064 89). This observation is in agreement with Grunwald's formula[16] which shows quantitatively how the disparity of progress lowers the energy barrier (in a symmetric reaction, $\Delta E^\circ = 0$ and according to eq 3 the energy barrier is equal to the intrinsic barrier $\Delta E^*_0$) by adding an extra term which has a negative sign. The $\tau$ value is associated with the electronegativity as we discussed earlier. Within each group, the more electronegative X is, the smaller $\tau$ is. In summary, the intrinsic barrier is large for sp-hybridized X. The intrinsic barrier is lowered by increasing the electronegativity of X and by increasing the excess contribution of configuration $\psi_3$ (in eq 7) to the transition state.

The present analysis may be compared with that of Shaik and Pross,[5,14] who classify reactions according to a $f$ factor. According to their definition, the $f$ factor is proportional to $W_R$ which accounts for the delocalization properties of the charge-transfer states. The intrinsic barrier is affected by the curvature factor $f$ as well as an energy gap factor ($I_{N:} - A_{RX}$), where $I$ and $A$ are the ionization potential and electron affinity, respectively. Herein, the reactions are classified according to the hybridization factor and the electronic structure of the TS as measured by the contribution of $\psi_3$ in eq 7. The intrinsic barriers are related to the

(22) Lowry, T. H.; Richardson, K. S. *Mechanism and Theory in Organic Chemistry*, 3rd ed.; Harper & Row: New York, 1987; p 381 and references therein.

**Table IV.** Intrinsic Barriers of Symmetric Reactions, Integrated Charge on X in $CH_3X$, and Basicity of $X^-$ in the Gas Phase and in Solution[a]

| X | $\Delta E^*_{0(XX)}$[b] (kJ/mol) | $-Q_X$ (e) | $pK_a$ | $\Delta H$ (kJ/mol) |
|---|---|---|---|---|
| H | 235.15 | -0.066 | 35 | 1676 |
| CCH | 213.82 | 0.290 | 24 | 1572 |
| CN | 191.02 | 0.328 | 9.21 | 1478 |
| NC | 130.24 | 0.650 | | |
| PH₂ | 147.67 | -0.515 | 29 | 1551 |
| SH | 110.83 | -0.003 | 7.0 | 1480 |
| Cl | 75.44 | 0.224 | -6 to -7 | 1395 |
| NH₂ | 145.30 | 0.350 | 32.5 | 1673 |
| OH | 98.49 | 0.545 | 15.7 | 1636 |
| OOH | 76.35 | 0.604 | 11.6[c] | |
| F | 52.70 | 0.626 | 3.18 | 1555 |

[a] The $pK_a$ and $\Delta H$ values are from ref 25a and 25b, respectively. $\Delta H$ is the enthalpy change of the reaction HX → $H^+$ + $X^-$ in the gas phase at 298 K. [b] In kJ/mol to be consistent with the units of $\Delta H$. [c] Data from ref 25c.

group to which the reaction belongs ($\omega$ value) and the electronegativity of X ($\tau$ value). The classification that we used is based on the relationship between $\Delta E^*_0$ and $\Delta E^\circ_c$. At first, it seems that our $\omega$ factor is similar to Shaik and Pross's $f$ factor, and our $\tau$ factor is similar to their $(I_{N:} - A_{RX})$ factor. However, quite different results were obtained from the two analyses. For example, according to their calculations,[5] CCH and OH have similar $f$ factors ($W_{R:} = 0.36$), F and Cl have similar $f$ factors ($W_{R:} \sim 0.24$–0.25), and $W_{R:} = 0.30$ for CN, whereas according to our analysis, CCH and CN belong to one group and OH and F belong to another group. Moreover, according to the Shaik and Pross model, the $\Delta E^*_0$ value for the symmetric reaction N = X = F is larger than that of the reaction N = X = Cl because the former has a larger energy gap factor ($I_{N:} - A_{RX}$). According to our model, there are two competing factors: the electronic structure factor ($\omega$ value) favors N = X = Cl, since it involves an excess $\psi_3$ contribution to the TS; however, the electronegativity factor ($\tau$ value) favors N = X = F. Depending on which factor dominates, the intrinsic barrier for F may be smaller or larger than that of Cl. Results obtained at the HF level[7a–c,23] show that the

N = X = Cl case has a smaller intrinsic barrier. However, results obtained at the MP2' and MP2 levels[7b,c] indicate that the N = X = F case has a smaller intrinsic barrier in agreement with recent configuration interaction calculations.[24]

Within each group, the intrinsic barrier $\Delta E^*_{0(XX)}$ is related to the charge ($Q_X$) on X in $CH_3X$ (see Table IV). As discussed above, $\Delta E^*_{0(XX)}$ is related to the electronegativity of X within each group. Since $Q_X$ is a measure of the electronegativity of X, the relationship between $\Delta E^*_{0(XX)}$ and $Q_X$ is not unexpected. Furthermore, within each group the intrinsic barrier is related to the base strength of $X^-$ (see $pK_a$ values in Table IV). As the base strength increases ($pK_a$ increases), the intrinsic barrier increases. This can be understood by the fact that the base strength of $X^-$ reflects the electron-donating ability of $X^-$. It is an indication of the electronegativity of X as well.

**Conclusions**

Chemical reactions are classified according to molecular and mechanistic criteria. In the case of the $S_N2$ reactions discussed in this paper, the reactions can be classified according to the hybridization of the leaving group (specifically, the atom adjacent to carbon) and the electronic structure of the TS. A sp-hybridized atom results in a rapid ascent or a large curvature of the reactant energy profile and a high intrinsic barrier. An excess contribution of $\psi_3$ to the TS in eq 7 lowers the intrinsic barrier. Within each group, the intrinsic barrier is related to the electronegativity of the leaving group. As the electronegativity of the leaving group increases, the intrinsic barrier decreases. Within each group there is a linear relationship between $\Delta E^*$ and $\Delta E^\circ_c$.

(23) Wolfe, S.; Mitchell, D. J.; Schlegel, H. B. *J. Am. Chem. Soc.* **1981,** *103,* 7694.

(24) Vetter, R.; Zülicke, L. *J. Am. Chem. Soc.* **1990,** *112,* 5136.
(25) (a) Reference 22, p 294, 297. (b) Bartmess, J. E.; Scott, J. A.; McIver, R. T., Jr. *J. Am. Chem. Soc.* **1979,** *101,* 6046. (c) Weast, R. C.; Lide, D. R.; Astle, M. J.; Beyer, W. H. *CRC Handbook of Chemistry and Physics,* 70th ed.; CRC Press: Boca Raton, FL, 1989, p D-165.

# The Fluorophosphoranyl Series: Theoretical Insights into Relative Stabilities and Localization of Spin

**Christopher J. Cramer**

*Contribution from the U.S. Army Chemical Research Development and Engineering Center, Research Directorate, Physics Division, Chemometric and Biometric Modeling Branch, Aberdeen Proving Ground, Maryland 21010-5423. Received May 9, 1990*

**Abstract:** The nine isomeric local minima within the complete fluorophosphoranyl series ($H_nPF_{4-n}^\bullet$, n = 0–4) have been investigated at the UHF/6-31G* and higher levels. Quantitative analysis of fluorine apicophilicity and hyperconjugative effects within the trigonal-bipyramidal series is presented. The ability of atomic orbitals on axially disposed fluorine atoms to participate in either a hyperconjugative donor or acceptor role is quite limited in comparison to analogous opportunities for equatorially disposed fluorine atoms. Decomposition of metathesis energy changes into apicophilic and hyperconjugative components permits rational evaluation of the corresponding equilibria. Localization of spin density is accomplished efficiently by using the calculated MP2/6-311G** electron density. Fermi contact integrals derived therefrom allow for highly accurate prediction of isotropic hyperfine coupling constants after application of a small scaling factor. Techniques alternatively using s-orbital spin density for such predictions are far less satisfactory.

Phosphoranyl radicals, first proposed as metastable reaction intermediates in 1957,[1] have been the subject of detailed study.

Implicated, inter alia, as playing a role in radiolytically damaged nucleic acid polymers, they have attracted considerable experi-